

Scaling in internally heated convection: a unifying theory

Qi Wang^{1,2}, Detlef Lohse^{1,3,*} and Olga Shishkina^{3†}

¹*Physics of Fluids Group and Max Planck Center for Complex Fluid Dynamics,*

MESA+ Institute and J. M. Burgers Centre for Fluid Dynamics,

University of Twente, P.O. Box 217,

7500AE Enschede, The Netherlands

²*Department of Modern Mechanics,*

University of Science and Technology of China, Hefei 230027, China

³*Max Planck Institute for Dynamics and Self-Organization, 37077 Göttingen, Germany*

(Dated: November 16, 2021)

Abstract

We offer a unifying theory for turbulent purely internally heated convection, generalizing the unifying theories of Grossmann and Lohse (2000, 2001) for Rayleigh–Bénard turbulence and of Shishkina, Grossmann and Lohse (2016) for turbulent horizontal convection, which are both based on the splitting of the kinetic and thermal dissipation rates in respective boundary and bulk contributions. We obtain the mean temperature of the system and the Reynolds number (which are the response parameters) as function of the control parameters, namely the internal thermal driving strength (called, when nondimensionalized, the Rayleigh–Roberts number) and the Prandtl number. The results of the theory are consistent with our direct numerical simulations.

Thermally driven turbulence is omnipresent in nature and technology. The thermal driving can be thanks to the temperature boundary conditions such as in Rayleigh–Bénard convection – a flow in a container heated from below and cooled from above [1–3] – or in horizontal convection [4–6] or vertical convection [7–10], where parts of the top, bottom, or sidewalls of the container are set at different temperatures. However, the thermal driving can also be thanks to internal heating, where the temperature field is driven by some forcing in the bulk. In many cases in nature, both ways of driving play a role at the same time. E.g., this holds for the Earth’s mantle due to the driving through the hot inner core of the Earth and an additional driving due to the decay of radioactive material inside the core, producing heat [11–18]. Thus, in the Earth’s mantle, about 10–20% of the heat is transferred from the core, while the rest occurs due to the internal heating [18]. The internal heating dominates also in the atmosphere of Venus [19, 20], which is heated up due to the absorption of sun light. One more example is the formation of Pluto’s polygonal terrain, which is caused not only by convection of Rayleigh–Bénard type [21, 22], but also by internally heated convection [23]. And, of course, internally heated convection is relevant in many engineering applications, e.g., liquid-metal batteries [24, 25].

To obtain a theoretical understanding of thermally driven turbulence including the cases of mixed thermal driving, it is mandatory to first understand the pure and well defined cases, namely on the one hand turbulent Rayleigh–Bénard convection (RBC, exclusively driven by the heated and cooled plates), and on the other hand turbulent purely internally heated convection (IHC, exclusively driven by thermal forcing of the temperature field in the bulk), see [26–29]. For the former case, Grossmann and Lohse (GL) have developed a unifying theory [30–34], with which the heat transfer and the degree of turbulence can quantitatively be described as function of the control parameters, in excellent agreement with the experimental and numerical data over a range of more than 7 orders of magnitude in the control parameters Ra and Pr . Later this theory was also extended to horizontal convection [5] (HC) and double diffusive convection [35]. GL arguments were also applied to IHC, to estimate the bulk temperature for small and moderate Pr [27]. A complete theory, however, does not yet exist for purely internally heated convection.

The objective of the present work is to apply the reasoning of GL’s theory to the case of purely internally heated convection and to develop a unifying theory for this case. In addition, we perform direct numerical simulations (DNS) of turbulent purely internally

heated convection over a large range of control parameters and compare the DNS results with the theoretical predictions. The DNS are conducted in two dimensions (2D), as (i) the theory is based on Prandtl's equations, which are also 2D in spirit, as (ii) 2D and 3D thermally driven turbulence show very close analogies with respect to the integral quantities, in particular for large Prandtl numbers $Pr \geq 1$ [36], and as (iii) otherwise, due to unavoidable limitations in available CPU time, we could explore only a much smaller portion of the parameter space.

In RBC, next to the geometric aspect ratio Γ of the sample (the ratio between lateral and vertical extensions), the control parameters of the system are the temperature difference between top and bottom wall (in dimensionless form, the Rayleigh number) and the ratio between kinematic viscosity ν and thermal diffusivity κ , namely the Prandtl number $Pr = \nu/\kappa$. The response of the system consists of the heat flux from bottom to top (in dimensionless form, the Nusselt number Nu) and the degree of turbulence (in dimensionless form, the Reynolds number Re). In IHC, instead of the Rayleigh number, the dimensionless driving strength Rr of the temperature field takes the role of the second control parameter, next to Pr . It is often called Rayleigh–Roberts number (and that is why we use the abbreviation Rr) and will be defined below. The main response parameter, next to Re , is the mean temperature which the bulk achieves thanks to the internal driving. This is related to the heat fluxes into the top and bottom plates; note that they are different from each other. So the objective of this paper is to explain how the mean temperature and the Reynolds number in turbulent IHC depend on Rr and Pr , for large enough aspect ratio Γ of the sample.

The flow in IHC is confined between two parallel plates with distance L , with the gravitational acceleration $\mathbf{g} \equiv -g\mathbf{e}_z$ acting orthogonally to these plates. The underlying dynamical equations within the Boussinesq approximation are the compressibility condition $\partial_i u_i = 0$, and

$$\partial_t u_i + u_j \partial_j u_i = -\partial_i p + \nu \partial_j^2 u_i + \beta g \delta_{iz} \theta, \quad (1)$$

$$\partial_t \theta + u_j \partial_j \theta = \kappa \partial_j^2 \theta + \Omega, \quad (2)$$

for the velocity field $\mathbf{u}(\mathbf{x}, t)$, the kinematic pressure field $p(\mathbf{x}, t)$, and the reduced temperature field $\theta(\mathbf{x}, t) \equiv T(\mathbf{x}, t) - T_{plate}$. Here T_{plate} is the temperature of both top and bottom plates, β is the thermal expansion coefficient, δ_{ij} the Kronecker delta and Ω the constant bulk

driving of the temperature field, which in non-dimensional form is called Rayleigh–Roberts number

$$Rr = \beta g L^5 \Omega / (\kappa^2 \nu). \quad (3)$$

The equations (1) and (2) are supplemented by the boundary conditions (BCs) $u_i = 0$ and $\theta = 0$ at both plates. Periodic BCs are used in the horizontal direction.

The main responses of the system can be expressed in terms of the mean temperature $\Delta \equiv \langle \theta(\mathbf{x}, t) \rangle_V$ achieved in the system, where the average $\langle \cdot \rangle_V$ is over volume and time. The nondimensional form of this response parameter is

$$\tilde{\Delta} \equiv \kappa \Delta / (\Omega L^2). \quad (4)$$

The other main nondimensional response parameter is the Reynolds number $Re = UL/\nu$, with $U \equiv \sqrt{\langle \mathbf{u}^2 \rangle_V}$.

Obviously, due to the internal heating, the heat flux

$$Q(z) \equiv \langle u_z \theta \rangle - \kappa \langle \partial_z \theta \rangle \quad (5)$$

(or in dimensionless form $\tilde{Q}(z) \equiv Q(z)/(\Omega L)$) in the system is not constant as in RBC, but depends on the height z . Here, $\langle \cdot \rangle$ means average in time and in a plane of constant z . However, a simple integration of eq. (2) over the full volume yields that the quantity

$$\tilde{Q}_0 \equiv z/L - \tilde{Q}(z) \quad (6)$$

is constant for all z and equals

$$\tilde{Q}_0 = -\tilde{Q}(z=0) = \frac{\kappa}{\Omega L} \langle \partial_z \theta \rangle|_{z=0} \geq 0. \quad (7)$$

\tilde{Q}_0 is thus a further dimensionless response parameter of the system. Eq. (7) implies that the dimensionless heat flux \tilde{Q} is non-positive at $z = 0$. Applying eq. (6) at $z = L$ gives the dimensionless flux at $z = L$,

$$\tilde{Q}(z=L) = -\frac{\kappa}{\Omega L} \langle \partial_z \theta \rangle|_{z=L} = 1 - \tilde{Q}_0 \geq 0, \quad (8)$$

Relations (7) and (8) immediately show that $0 \leq \tilde{Q}_0 \leq 1$.

As it is well known [1, 37], in RBC exact relations between the time and volume averaged thermal and kinetic dissipation rates, $\epsilon_\theta \equiv \kappa \langle (\partial_i \theta(\mathbf{x}, t))^2 \rangle_V$ and $\epsilon_u \equiv \nu \langle (\partial_i u_j(\mathbf{x}, t))^2 \rangle_V$, and

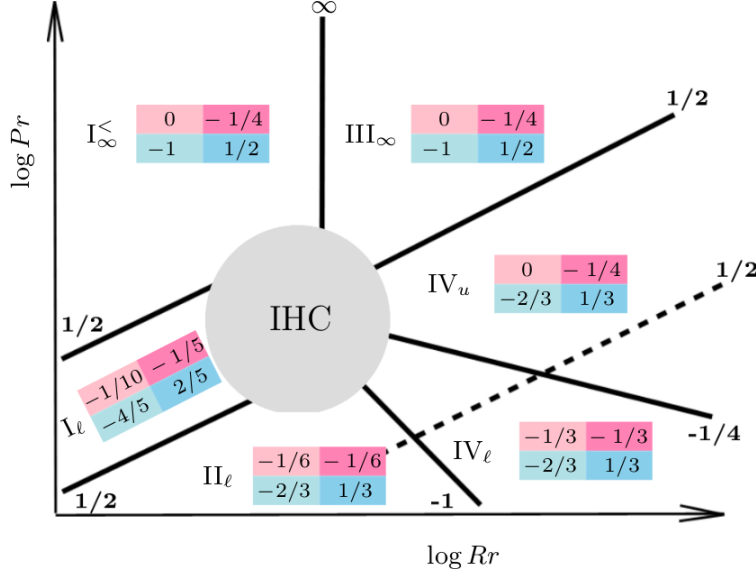


FIG. 1. Sketch of the phase space of IHC with the various limiting scaling regimes following from our unifying theory. Continuous lines show the slopes of the transitions between the different regimes. The exponent β_0 of each slope $Pr \sim Rr^{\beta_0}$ between the different regimes in phase space is written in bold, close to the corresponding line. The dashed line shows the slope of the transition to the ultimate regime. For each regime, the color box represents the scaling exponents in the scalings of $\tilde{\Delta}$ and Re versus Pr and Rr : $\begin{cases} \tilde{\Delta} \sim Pr^{\beta_1} Rr^{\beta_2} \\ Re \sim Pr^{\beta_3} Rr^{\beta_4} \end{cases}$. This phase space for IHC is the analogous one to the one of RBC of [31] and the one of HC in [5].

the dimensionless control and response parameters Nu , Ra , and Pr can be obtained from multiplying the thermal advection equation with $\theta(\mathbf{x}, t)$ and the Navier–Stokes equation with $u_i(\mathbf{x}, t)$ and subsequent Gauss integration and time and space averaging. Here we apply the same procedure to Eqs. (2) and (1) and obtain

$$\epsilon_\theta = \Omega \Delta = \frac{L^2}{\kappa} \Omega^2 \tilde{\Delta} = \frac{\kappa \Delta^2}{L^2} \tilde{\Delta}^{-1}, \quad (9)$$

$$\epsilon_u = \frac{\nu^3}{L^4} Rr Pr^{-2} \left(\frac{1}{2} - \tilde{Q}_0 \right). \quad (10)$$

As $\epsilon_u \geq 0$ is non-negative by definition, we can now further restrain the magnitude of the dimensionless heat flux through the bottom plate: $0 \leq \tilde{Q}_0 \leq 1/2$. Just as the corresponding relations in RBC, also here, Eqs. (9) and (10) relate the averaged thermal and kinetic dissipation rates with the dimensionless control (Rr , Pr) and response ($\tilde{\Delta}$, \tilde{Q}_0) parameters.

The key idea of the GL theory [30, 31] is to split the kinetic and thermal dissipation rates

Regime	$\epsilon_u/(\nu^3 L^{-4}) \sim Pr^{-2} Rr$	$\epsilon_\theta/(\kappa \Delta^2 L^{-2}) \sim \tilde{\Delta}^{-1}$	$\tilde{\Delta}$	Re
$I_\infty^<$	$\sim Re^2$	$\sim Pr^{1/2} Re^{1/2}$	$\sim Pr^0 Rr^{-1/4}$	$\sim Pr^{-1} Rr^{1/2}$
I_u	$\sim Re^{5/2}$	$\sim Pr^{1/3} Re^{1/2}$	$\sim Pr^{1/15} Rr^{-1/5}$	$\sim Pr^{-4/5} Rr^{2/5}$
I_ℓ	$\sim Re^{5/2}$	$\sim Pr^{1/2} Re^{1/2}$	$\sim Pr^{-1/10} Rr^{-1/5}$	$\sim Pr^{-4/5} Rr^{2/5}$
II_ℓ	$\sim Re^3$	$\sim Pr^{1/2} Re^{1/2}$	$\sim Pr^{-1/6} Rr^{-1/6}$	$\sim Pr^{-2/3} Rr^{1/3}$
III_∞	$\sim Re^2$	$\sim Pr Re \tilde{\Delta}$	$\sim Pr^0 Rr^{-1/4}$	$\sim Pr^{-1} Rr^{1/2}$
IV_u	$\sim Re^3$	$\sim Pr Re^{3/2} \tilde{\Delta}$	$\sim Pr^0 Rr^{-1/4}$	$\sim Pr^{-2/3} Rr^{1/3}$
IV_ℓ	$\sim Re^3$	$\sim Pr Re$	$\sim Pr^{-1/3} Rr^{-1/3}$	$\sim Pr^{-2/3} Rr^{1/3}$

TABLE I. Scalings of ϵ_u , ϵ_θ , Re and $\tilde{\Delta}$ in the different limiting regimes in IHC.

into contributions from the corresponding boundary layers (BLs) and bulks,

$$\epsilon_u = \epsilon_{u,\text{BL}} + \epsilon_{u,\text{bulk}}, \quad \epsilon_\theta = \epsilon_{\theta,\text{BL}} + \epsilon_{\theta,\text{bulk}},$$

and to apply the respective scaling relations for those (i.e., for $\epsilon_{u,\text{BL}}$, $\epsilon_{u,\text{bulk}}$, $\epsilon_{\theta,\text{BL}}$ and $\epsilon_{\theta,\text{bulk}}$), based on boundary layer theory and Kolmogorov's theory for fully developed turbulence in the bulk. The introduced scaling regimes I, II, III, and IV correspond to BL–BL, bulk–BL, BL–bulk, and bulk–bulk dominance in ϵ_u and ϵ_θ , respectively. Here one should also take into account mean thicknesses of the thermal BLs (λ_θ) and viscous BLs (λ_u). The cases $\lambda_\theta < \lambda_u$ (large Pr) and $\lambda_\theta > \lambda_u$ (small Pr) correspond to different scaling regimes, and therefore we assign the subscripts u and ℓ to regimes I, II, III and IV, which indicate the *upper-Pr* and *lower-Pr* cases, respectively. Equating ϵ_u and ϵ_θ to their estimated either bulk or BL contributions and employing the classical Prandtl scaling relations for the BL thicknesses λ_θ and λ_u [38], one in principle obtains eight theoretically possible scaling regimes. Regimes II_u and III_ℓ are rather small, because, e.g., in II_u , it is expected that $\lambda_\theta \geq \lambda_u$ due to the BL-dominance in ϵ_θ , but on the other hand, $\lambda_\theta \leq \lambda_u$ should hold due to the large Pr . By similar arguments, regime III_ℓ is also small.

The mean thicknesses of the BLs are estimated as follows: $\lambda_u \sim L/\sqrt{Re}$, as in RBC [30, 31, 39, 40], and $\lambda_\theta \equiv 2/(\lambda_{\theta,\text{top}}^{-1} + \lambda_{\theta,\text{bottom}}^{-1})$. Approximating $\langle \partial_z \theta \rangle$ at $z = 0$ and $z = H$ with the ratio of Δ and the top and bottom thermal BL thicknesses, $\lambda_{\theta,\text{top}}$ and $\lambda_{\theta,\text{bottom}}$, from Eqs. (4), (7) and (8) we obtain $\lambda_\theta \sim L\tilde{\Delta}$.

The value of $\epsilon_{u,\text{bulk}}$ is estimated as

$$\epsilon_{u,\text{bulk}} \sim U \frac{U^2}{L} \frac{L - \lambda_u}{L} \approx \frac{U^3}{L} = \frac{\nu^3}{L^4} Re^3,$$

which is relevant in the ϵ_u -bulk dominating regimes II_ℓ , IV_ℓ and IV_u , while the value of $\epsilon_{\theta,\text{bulk}}$ is estimated as

$$\epsilon_{\theta,\text{bulk}} \sim U \frac{\Delta^2}{L} \frac{L - \lambda_\theta}{L} \approx \frac{U \Delta^2}{L} = \frac{\kappa \Delta^2}{L^2} Pr Re,$$

which is relevant in the ϵ_θ -bulk dominating regime IV_ℓ . For large Pr (regimes III_u and IV_u), the thermal BL is embedded into the kinetic one and therefore in eq. (11), the magnitude of the velocity of the flow, which carries the temperature in the bulk, is reduced from U to $(\lambda_\theta/\lambda_u)U$, leading to

$$\epsilon_{\theta,\text{bulk}} \sim \frac{\lambda_\theta}{\lambda_u} \frac{U \Delta^2}{L} \frac{L - \lambda_\theta}{L} \approx \frac{\kappa \Delta^2}{L^2} Pr Re^{3/2} \tilde{\Delta}. \quad (11)$$

The kinetic dissipation rate in the BL is $\sim \nu(U/\lambda_u)^2$. Hence,

$$\epsilon_{u,\text{BL}} \sim \nu \frac{U^2}{\lambda_u^2} \frac{\lambda_u}{L} = \frac{\nu^3}{L^4} Re^{5/2}, \quad (12)$$

which is relevant in the ϵ_u -BL dominating regimes I_ℓ , I_u and III_u . As in [30, 31], the factor λ_u/L accounts for the volume fraction of the kinetic BL. With increasing Pr , λ_u saturates to $\sim L$, so this factor becomes one (just as argued in [31]), which yields

$$\epsilon_{u,\text{BL}} \sim \nu \frac{U^2}{\lambda_u^2} = \frac{\nu^3}{L^4} Re^2. \quad (13)$$

For small Ra or very large Pr , this leads to special regimes I_∞ and III_∞ on top of, respectively, I_u and III_u . In III_∞ , also $\epsilon_{\theta,\text{bulk}}$ scales differently to (11), namely as

$$\epsilon_{\theta,\text{bulk}} \sim \frac{\lambda_\theta}{L} \frac{U \Delta^2}{L} \frac{L - \lambda_\theta}{L} \approx \frac{\kappa \Delta^2}{L^2} Pr Re \tilde{\Delta}.$$

The thermal dissipation rate in the BL scales as $\sim \kappa(\Delta/\lambda_\theta)^2$, which is relevant in the ϵ_θ -BL dominating regimes I_ℓ , I_u , I_∞ and II_ℓ . This (again with the volume fraction factor) leads to

$$\epsilon_{\theta,\text{BL}} \sim \kappa \frac{\Delta^2}{\lambda_\theta^2} \frac{\lambda_\theta}{L} = \kappa \frac{\Delta^2}{L^2} \frac{\lambda_u}{\lambda_\theta} Re^{1/2}. \quad (14)$$

In the limiting regimes I_ℓ , II_ℓ and I_∞ , it holds $\lambda_u/\lambda_\theta \sim Pr^{1/2}$ [41, 42], while in regime I_u it holds $\lambda_u/\lambda_\theta \sim Pr^{1/3}$, all just as in the classical Prandtl–Blasius–Pohlhausen theory [38].

Equating ϵ_u and ϵ_θ to their estimated bulk or BL contributions, we obtain the scalings of $\tilde{\Delta}$ and Re in IHC, which are summarized in Tab. I and sketched in Fig. 1.

As already mentioned above, the very same idea was already applied to horizontal convection [5]. Interestingly enough, even a formal analogy between IHC and HC exists, out of which we could have already derived the scaling relations of Table I and Fig. 1. The reason for this formal analogy is that the relations obtained for ϵ_θ and ϵ_u (see Eqs. (5) and (6) of [5]) formally resemble the corresponding relations (9) and (10) here. For the first equation this becomes particular obvious when writing $\epsilon_\theta = \frac{L^2}{\kappa} \Omega^2 \tilde{\Delta} = \frac{\kappa}{L^2} \Delta^2 \tilde{\Delta}^{-1}$ and for the second when realizing that $(\frac{1}{2} - \tilde{Q}_0)$ is only a dimensionless factor between 0 and 1/2. Then one sees immediately that the role of the control parameter Ra in HC is taken by that of the control parameter R in IHC and the role of the response parameter Nu in HC is taken by that of the (inverse) response parameter $\tilde{\Delta}^{-1}$ in IHC. All derived scaling relations in the different limiting regimes of HC can directly be taken over. The corresponding values for IHC give the same results as obtained above and have already been shown in Table I and Fig. 1.

To check these predictions of the GL theory generalized to IHC, we have performed 2D DNS according to Eqs. (1) and (2) with the corresponding BCs. We chose an aspect ratio of $\Gamma = 2$ for the laterally periodic box. The numerics have been validated by making sure that the exact relations (10) are fulfilled. Simulations were performed using the second-order staggered finite difference code AFiD [43, 44]. This code has already been extensively used to study RBC, see, e.g. [45, 46].

The parameter combinations (Rr, Pr) for which we performed simulations are shown in the parameter space of Fig. 2a. A typical snapshot of the temperature field together with the mean temperature profile for one parameter combination are displayed in Fig. 2b. One can see the stably-stratified layer near the bottom plate. The interaction of the upper convection zone and the lower stably-stratified region leads to the so-called penetrative convection [47, 48]. The mean temperature profile, which, as expected and typical for IHC, displays top-down asymmetry.

The results for the response parameters $\tilde{\Delta}$ and Re as functions of the control parameters Rr and Pr are shown in Figs. 3 and 4. As can be seen, in general, there are no pure scaling laws over the simulated range, but smooth crossovers from one regime to the other, very similarly as in RBC [34], reflecting the key idea of the unifying theory by [30, 31]. We first discuss the dependences for the dimensionless mean temperature $\tilde{\Delta}$, see Figs. 3a, b. As a function of Pr (Fig. 3b), for all Rr the transition from $\tilde{\Delta} \sim Pr^{-1/10}$ of regime I_l to the

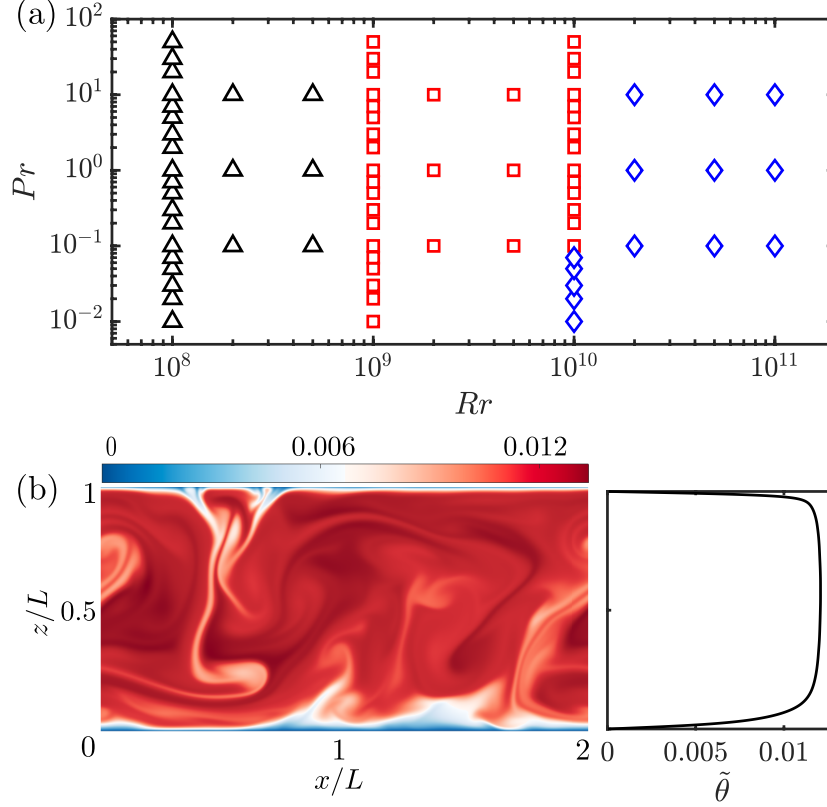


FIG. 2. (a) Rr vs. Pr parameter space of the simulated cases. Symbols denote the different grid resolutions used in DNS: 512×256 (\triangle), 1024×512 (\square), 2048×1024 (\diamond). (b) Instantaneous temperature field (color coded) and mean temperature profile for $Rr = 10^{10}$ and $Pr = 1$.

Pr -independence of regime $I_\infty^<$ can clearly be seen. The more turbulent regimes $IV_{u,\ell}$ are not yet realized, as the driving is not strong enough. This is also reflected in the Rr dependence $\tilde{\Delta} \sim Rr^{-1/5}$ reflecting that of regimes $I_{u,\ell}$. No indication to a stronger dependence as typical for the more turbulent regimes $IV_{u,\ell}$ can yet be seen. This is also seen in the dependences of the Reynolds number (Fig. 3 c, d): For small $Pr \leq 1$, it goes like $Re \sim Rr^{2/5}$ as in regimes $I_{u,\ell}$. For large $Pr = 10$ the results are consistent with $Re \sim Rr^{1/2}$ as in regime $I_\infty^<$. This scaling should go hand in hand with the scaling $\tilde{\Delta} \sim Rr^{-1/4}$ for the dimensionless mean temperature, but as seen from Fig. 3a, those data are presumably better described by $\tilde{\Delta} \sim Rr^{-1/5}$. Finally, on the Pr -dependence of Re : As seen from Fig. 3d, for all Rr the data show a transition from the $Re \sim Pr^{-4/5}$ scaling of regimes $I_{u,\ell}$ to the $Re \sim Pr^{-1}$ scaling of regime $I_\infty^<$, consistent with the corresponding transition for $\tilde{\Delta}$ in Fig. 3b.

All these results are consistent with our unifying theory, which however goes much beyond

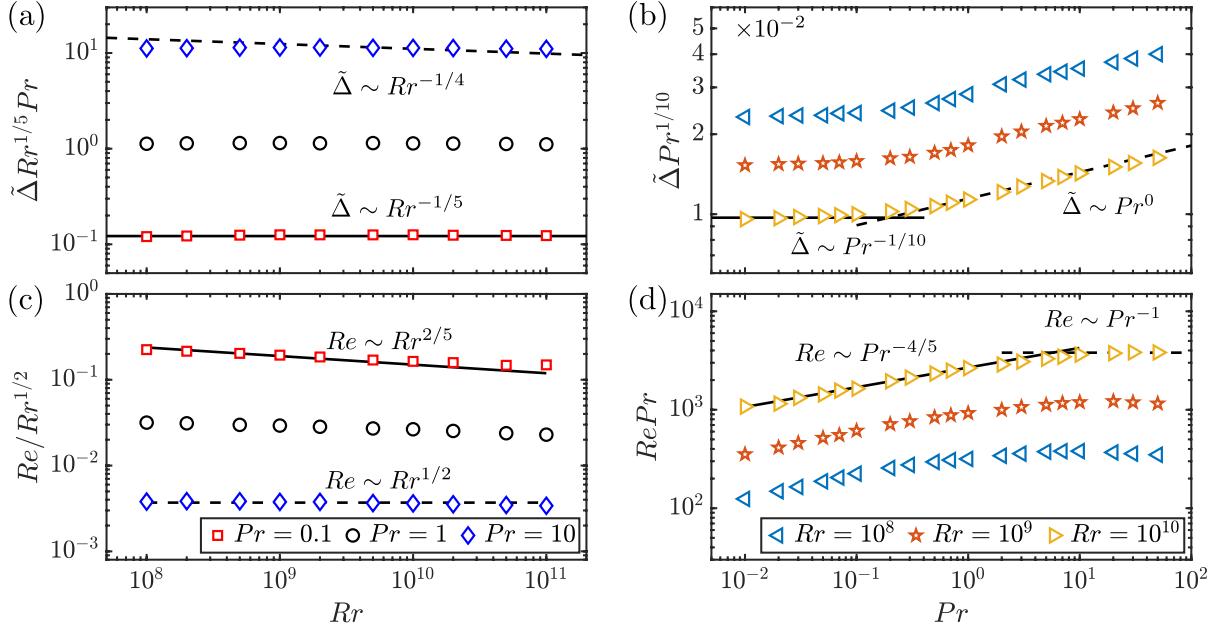


FIG. 3. Response parameters $\tilde{\Delta}$ (the dimensionless mean temperature of the bulk) and Re as function of the control parameters Rr and Pr : (a) Compensated $\tilde{\Delta}$ as function of Rr for fixed $Pr = 10^{-1}, 1, 10$. (b) Compensated $\tilde{\Delta}$ as function of Pr for fixed $Rr = 10^8, 10^9, 10^{10}$. (c) Compensated Re as function of Rr for fixed $Pr = 10^{-1}, 1, 10$. (d) $Re Pr$ as function of Pr for fixed $Rr = 10^8, 10^9, 10^{10}$. The straight lines with the corresponding scaling laws are added as guide to the eye.

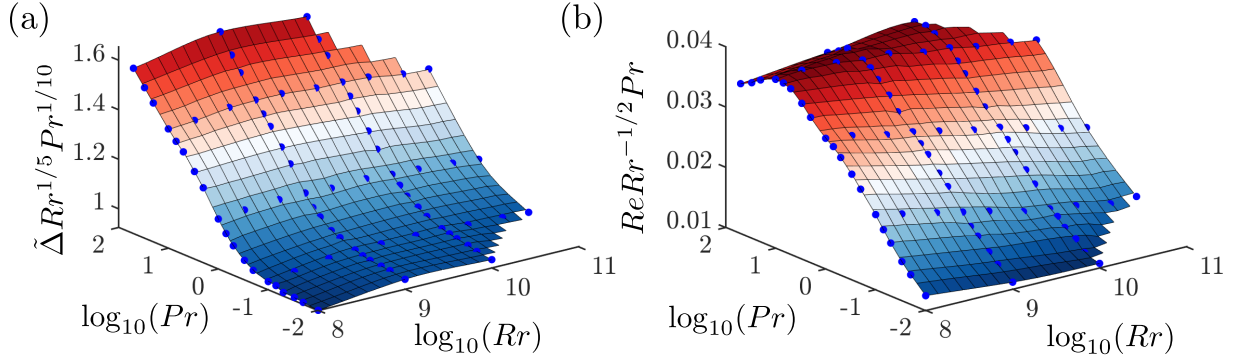


FIG. 4. Compensated three-dimensional visualization of (a) $\tilde{\Delta}(Rr, Pr)$ and (b) $Re(Rr, Pr)$.

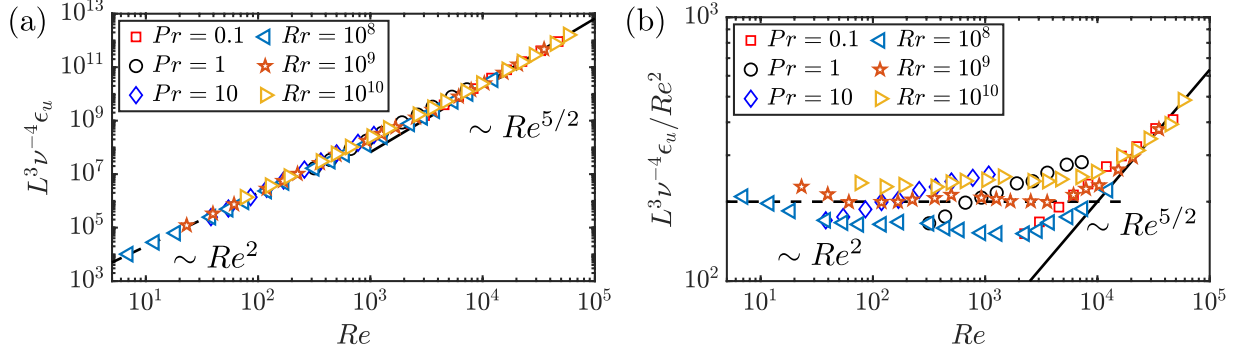


FIG. 5. The non-dimensionalized (a) absolute kinetic energy dissipation rate $L^3 \nu^{-4} \epsilon_u$ and (b) compensated kinetic energy dissipation rate $L^3 \nu^{-4} \epsilon_u / Re^2$ as function of Re . Note that $L^3 \nu^{-4} \epsilon_u \sim Rr Pr^{-2}$, Eq. 10, holds exactly throughout and has numerically been checked for consistency (not shown). Also note that the non-dimensionalized thermal energy dissipation rate (middle column of Table I) is nothing else but $\sim \tilde{\Delta}^{-1}$ and has thus already been shown in Figs. 2 a, b.

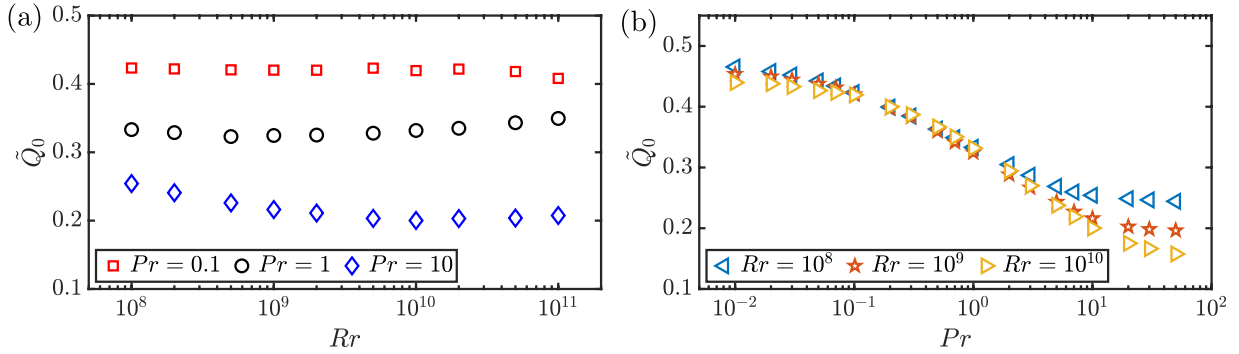


FIG. 6. Magnitude of the dimensionless heat flux through the bottom plate, \tilde{Q}_0 , as function of (a) Rr for the different Pr and (b) Pr for the different Rr (also shown in legends).

the simulated parameter range into the regimes in which the kinetic and thermal energy dissipation rates are dominated by the turbulent bulk contributions. These regimes are inaccessible with our present numerical simulations, even in 2D.

As an additional check of our unifying theory we also plot the kinetic energy dissipation rate as function of Re , see Fig. 5. Indeed, we find $\epsilon_u / (L^3 \nu^{-4}) \sim Re^{5/2}$ and $\sim Re^2$ as characteristic for the kinetic BL dominated regimes $I_{u,\ell}$ and $I_\infty^<$, consistent with what we have seen in Fig. 2.

Another (less important) response parameter of IHC is the magnitude of the dimensionless

heat flux \tilde{Q}_0 through the bottom plate. The numerical results for \tilde{Q}_0 are shown in Fig. 4. One sees from Fig. 4a that \tilde{Q}_0 only weakly depends on Rr in the present parameter range; this behaviour has also been found before in [28]. Fig. 4b illustrates that much less heat is transported outwards from the bottom plate with increasing Pr . The small \tilde{Q}_0 for large Pr is due to the less efficient shear-driven mixing of the fluid near the bottom plate.

In conclusion, in the spirit of the prior unifying theories for RBC [30, 31] and for HC [5], in this paper we have developed a unifying theory of IHC for the scaling of the mean temperature and the Reynolds number as functions of the control parameters Rr and Pr . The main result is visualized in Fig. 1. We have shown that the 2D DNS results are consistent with this theory, though the numerically accessible regimes are still dominated by the boundary layers, and not all predictions of the theory can already be tested at this point. Also 3D DNS are still outstanding. We have furthermore pointed towards the formal analogy between IHC and HC and it will be illuminating to explore this analogy also numerically.

Acknowledgements: R. Verzicco, D. Goluskin and K. L. Chong are gratefully acknowledged for discussions and support. We also acknowledge the Twente Max-Planck Center, the Deutsche Forschungsgemeinschaft (Priority Programme SPP 1881 "Turbulent Superstructures"). The simulations were carried out on the national e-infrastructure of SURFsara, a subsidiary of SURF cooperation, the collaborative ICT organization for Dutch education and research. Q.W. acknowledges financial support from China Scholarship Council (CSC) and Natural Science Foundation of China under grant no. 11621202.

D.L. and O.S. contributed equally to this work.

* d.lohse@utwente.nl

† Olga.Shishkina@ds.mpg.de

- [1] G. Ahlers, S. Grossmann, and D. Lohse, *Heat transfer and large scale dynamics in turbulent Rayleigh-Bénard convection*, Rev. Mod. Phys. **81**, 503 (2009).
- [2] D. Lohse and K.-Q. Xia, *Small-scale properties of turbulent Rayleigh-Bénard convection*, Annu. Rev. Fluid Mech. **42**, 335 (2010).
- [3] F. Chilla and J. Schumacher, *New perspectives in turbulent Rayleigh-Bénard convection*, Eur. Phys. J. E **35**, 58 (2012).

- [4] G. O. Hughes and R. W. Griffiths, *Horizontal convection*, Annu. Rev. Fluid Mech. **40**, 185 (2008).
- [5] O. Shishkina, S. Grossmann, and D. Lohse, *Heat and momentum transport scalings in horizontal convection*, Geophys. Res. Lett. **43**, 1219 (2016).
- [6] O. Shishkina and S. Wagner, *Prandtl-number dependence of heat transport in laminar horizontal convection*, Phys. Rev. Lett. **116**, 024302 (2016).
- [7] O. Shishkina, *Momentum and heat transport scalings in laminar vertical convection*, Phys. Rev. E **93**, 051102(R) (2016).
- [8] C. S. Ng, A. Ooi, D. Lohse, and D. Chung, *Vertical natural convection: application of the unifying theory of thermal convection*, J. Fluid. Mech. **764**, 349 (2015).
- [9] C. S. Ng, A. Ooi, D. Lohse, and D. Chung, *Changes in the boundary-layer structure at the edge of the ultimate regime in vertical natural convection*, J. Fluid Mech. **825**, 550 (2017).
- [10] C. S. Ng, A. Ooi, D. Lohse, and D. Chung, *Bulk scaling in wall-bounded and homogeneous vertical natural convection*, J. Fluid Mech. **841**, 825 (2018).
- [11] G. Houseman, *The dependence of convection planform on mode of heating*, Nature **332**, 346 (1988).
- [12] D. Bercovici, G. Schubert, and G. A. Glatzmaier, *Three-dimensional spherical models of convection in the Earth's mantle*, Science **244**, 950 (1989).
- [13] P. J. Tackley, D. J. Stevenson, G. A. Glatzmaier, and G. Schubert, *Effects of an endothermic phase transition at 670 km depth in a spherical model of convection in the Earth's mantle*, Nature **361**, 699 (1993).
- [14] H.-P. Bunge, M. A. Richards, and J. R. Baumgardner, *Effect of depth-dependent viscosity on the planform of mantle convection*, Nature **379**, 436 (1996).
- [15] T. Lay, J. Hernlund, and B. A. Buffett, *Core–mantle boundary heat flow*, Nature Geosci. **1**, 25 (2008).
- [16] W. B. Moore and A. A. G. Webb, *Heat-pipe earth*, Nature **501**, 501 (2013).
- [17] C. Mallard, N. Coltice, M. Seton, R. D. Müller, and P. J. Tackley, *Subduction controls the distribution and fragmentation of Earth's tectonic plates*, Nature **535**, 140 (2016).
- [18] G. Schubert, D. L. Turcotte, and P. Olson, *Mantle convection in the Earth and planets* (Cambridge University Press, ADDRESS, 2001).
- [19] D. J. Tritton and M. N. Zarraga, *Convection in horizontal layers with internal heat generation*.

- Experiments*, J. Fluid Mech. **30**, 21 (1967).
- [20] D. Tritton, *Internally heated convection in the atmosphere of Venus and in the laboratory*, Nature **257**, 110 (1975).
 - [21] W. B. McKinnon, F. Nimmo, T. Wong, P. M. Schenk, O. L. White, J. H. Roberts, J. M. Moore, J. R. Spencer, A. D. Howard, O. M. Umurhan, *et al.*, *Convection in a volatile nitrogen-ice-rich layer drives Pluto’s geological vigour*, Nature **534**, 82 (2016).
 - [22] A. J. Trowbridge, H. J. Melosh, J. K. Steckloff, and A. M. Freed, *Vigorous convection as the explanation for Pluto’s polygonal terrain*, Nature **534**, 79 (2016).
 - [23] K. Vilella and F. Deschamps, *Thermal convection as a possible mechanism for the origin of polygonal structures on Pluto’s surface*, J. Geophys. Res: Planets **122**, 1056 (2017).
 - [24] H. Kim, D. A. Boysen, J. M. Newhouse, B. L. Spatocco, B. Chung, P. J. Burke, D. J. Bradwell, K. Jiang, A. A. Tomaszowska, K. Wang, *et al.*, *Liquid metal batteries: past, present, and future*, Chem. Rev. **113**, 2075 (2013).
 - [25] L. Xiang and O. Zikanov, *Subcritical convection in an internally heated layer*, Phys. Rev. Fluids **2**, 063501 (2017).
 - [26] P. H. Roberts, *Convection in horizontal layers with internal heat generation. Theory*, J. Fluid. Mech. **30**, 33 (1967).
 - [27] D. Goluskin and E. A. Spiegel, *Convection driven by internal heating*, Phys. Lett. A **377**, 83 (2012).
 - [28] D. Goluskin and E. P. van der Poel, *Penetrative internally heated convection in two and three dimensions*, J. Fluid Mech. **791**, R6 (2016).
 - [29] K. Vilella, A. Limare, C. Jaupart, C. G. Farnetani, L. Fourel, and E. Kaminski, *Fundamentals of laminar free convection in internally heated fluids at values of the Rayleigh–Roberts number up to 10^9* , J. Fluid. Mech. **846**, 966 (2018).
 - [30] S. Grossmann and D. Lohse, *Scaling in thermal convection: A unifying view*, J. Fluid. Mech. **407**, 27 (2000).
 - [31] S. Grossmann and D. Lohse, *Thermal convection for large Prandtl number*, Phys. Rev. Lett. **86**, 3316 (2001).
 - [32] S. Grossmann and D. Lohse, *Prandtl and Rayleigh number dependence of the Reynolds number in turbulent thermal convection*, Phys. Rev. E **66**, 016305 (2002).
 - [33] S. Grossmann and D. Lohse, *Fluctuations in turbulent Rayleigh–Bénard convection: The role*

- of plumes*, Phys. Fluids **16**, 4462 (2004).
- [34] R. J. A. M. Stevens, E. P. van der Poel, S. Grossmann, and D. Lohse, *The unifying theory of scaling in thermal convection: the updated prefactors*, J. Fluid Mech. **730**, 295 (2013).
 - [35] Y. Yang, R. Verzicco, and D. Lohse, *Two-scalar turbulent Rayleigh-Bénard convection: Numerical simulations and unifying theory*, J. Fluid Mech. **848**, 648 (2018).
 - [36] E. P. van der Poel, R. J. A. M. Stevens, and D. Lohse, *Comparison between two- and three-dimensional Rayleigh-Bénard convection*, J. Fluid Mech. **736**, 177 (2013).
 - [37] B. I. Shraiman and E. D. Siggia, *Heat transport in high-Rayleigh number convection*, Phys. Rev. A **42**, 3650 (1990).
 - [38] H. Schlichting, *Boundary layer theory*, 7th ed. (McGraw Hill, New York, 1979).
 - [39] O. Shishkina, S. Horn, S. Wagner, and E. S. C. Ching, *Thermal boundary layer equation for turbulent Rayleigh-Bénard convection*, Phys. Rev. Lett. **114**, 114302 (2015).
 - [40] E. S. C. Ching, H. S. Leung, L. Zwirner, and O. Shishkina, *Velocity and thermal boundary layer equations for turbulent Rayleigh-Bénard convection*, Phys. Rev. Research **1**, 033037 (2019).
 - [41] H. Schlichting and K. Gersten, *Boundary layer theory*, 8th ed. (Springer Verlag, Berlin, 2000).
 - [42] O. Shishkina, M. Emran, S. Grossmann, and D. Lohse, *Scaling relations in large-Prandtl-number natural thermal convection*, Phys. Rev. Fluids **2**, 103502 (2017).
 - [43] R. Verzicco and P. Orlandi, *A finite-difference scheme for three-dimensional incompressible flows in cylindrical coordinates*, J. Comput. Phys. **123**, 402 (1996).
 - [44] van der Poel, E. P. and Ostilla-Mónico, R. and Donners, J. and Verzicco, R., *A pencil distributed finite difference code for strongly turbulent wall-bounded flows*, Comput. Fluids **116**, 10 (2015).
 - [45] Q. Wang, R. Verzicco, D. Lohse, and O. Shishkina, *Multiple states in turbulent large-aspect ratio thermal convection: What determines the number of convection rolls?*, Phys. Rev. Lett. **125**, 074501 (2020).
 - [46] Q. Wang, K.-L. Chong, R. J. A. M. Stevens, R. Verzicco, and D. Lohse, *From zonal flow to convection rolls in Rayleigh-Bénard convection with free-slip plates*, J. Fluid. Mech. (In Press) (2020).
 - [47] G. Veronis, *Penetrative Convection.*, Astrophys. J. **137**, 641 (1963).
 - [48] Q. Wang, Q. Zhou, Z.-H. Wan, and D.-J. Sun, *Penetrative turbulent Rayleigh-Bénard convection in two and three dimensions*, J. Fluid. Mech. **870**, 718 (2019).